Modeling of Centrifuge Filtration System for Severe Accident Source Term Treatment

Shuchang Liu[a], Man-Sung Yim[a*]
[a]*Department of Nuclear and Quantum Engineering, Korea Advanced Institute of Science and Technology*
**Corresponding author: msyim@kaist.ac.kr*

1. Introduction

Reactor containment may lose its structural integrity due to over-pressurization during a severe accident. This can lead to uncontrolled radioactive releases to the environment. For preventing the dispersion of these uncontrolled radioactive releases to the environment, several ways to capture or mitigate these radioactive source term releases are under investigation at KAIST. Such technologies are based on concepts like a vortex- like air curtain, a chemical spray, and a suction arm. Treatment of the radioactive material captured by these systems would be required, before releasing to environment.

For current filtration systems in the nuclear industry, IAEA lists sand, multi-venturi scrubber, high efficiency particulate arresting (HEPA), charcoal and combinations of the above in NS-G-1-10, 4.143. For example, AREVA has used multi-venturi scrubbers for a wet style FCVS and Worley Parsons has developed a dry filtered venting solution using HEPA filters.

However, centrifuges are one of the traditional separators, which was not included in the aforementioned list.

Centrifuge, or cyclone, has long been used in industry for gas cleaning and removing solids or liquids from particle laden flows. The basic principle is that gas flows are introduced into the system via tangential inlets. Centrifugal forces act on particulates or aerosols suspended in the gas, which are drawn toward the cyclone wall.

Considering the flexibility and high efficiency, a centrifuge combined with a multi modular absorbent filtration system is being proposed in this paper. The numerical model is discussed in this paper.

The conceptual design is shown below.

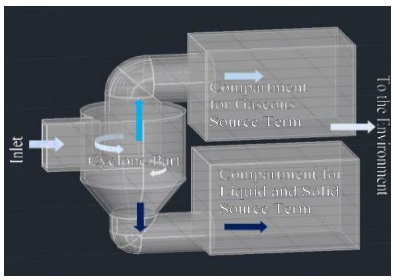

Fig. 1. Conceptual design and work flow of proposed centrifugal filtration system for source term treatment.

2. Governing equations

The source term focuses on the radioactive noble gases, typically xenon and krypton, and radioactive iodine. The released radioactive iodine is 91% gaseous I_2, 5% iodine-bearing particulate, and 4% a gaseous organic iodine compound. Except for iodine and the noble gases, the radioactive materials released to the containment are taken to be aerosol particles [1].

To analyze the two phase (gas and particle) source term, the governing equations are listed [2][3].

2.1 Continuum phase

The continuity equation for the gaseous part with no interphase mass transfer is

$$\frac{\partial \theta_f}{\partial t} + \nabla \cdot \left(\theta_f \boldsymbol{u}_f\right) = 0 \quad (1)$$

Where $\boldsymbol{u}_f$ is the gas velocity and θ_f is the gas volume fraction.

The momentum equation for the gas is

$$\frac{\partial (\theta_f \boldsymbol{u}_f)}{\partial t} + \nabla \cdot \left(\theta_f \boldsymbol{u}_f \boldsymbol{u}_f\right) = -\frac{1}{\rho_f}\nabla p - \frac{1}{\rho_f}\boldsymbol{F} + \theta_f \mathbf{g} \quad (2)$$

where ρ_f is gas density, p is gas pressure, and g is the gravitational acceleration. F is the rate of momentum exchange per volume between the gas and particle phases. For simplification, the gas phase is incompressible and gas and particle phases are isothermal. No mass transfer between the phases, no lift force and no virtual mass force are assumed. The momentum equation presented here neglects viscous molecular diffusion in the gas but retains the viscous drag between particles and gas through the interphase drag force, F.

2.2 Particulate phase

The dynamics of the particle phase is described using the particle probability distribution function ϕ ($\boldsymbol{x}$, $\boldsymbol{u}_p$, ρ_p, Ω_p, t) where $\boldsymbol{x}$ is the particle volume, $\boldsymbol{u}_p$ is the particle velocity, ρ_p is the particle density and Ω_p is the particle volume. For the present it is assumed that the mass of each particle is constant in time (no mass transfer between particles or to the fluid), but particles may have a range of sizes and densities. The

time evolution of φ is obtained by solving a Liouville equation for the particle distribution function [4],

$$\frac{\partial \phi}{\partial t} + \nabla \cdot (\phi \boldsymbol{u}_p) + \nabla_{\boldsymbol{u}_p} \cdot (\phi \boldsymbol{A}) = 0 \quad (3)$$

where $\nabla_{\boldsymbol{u}_p}$ is the divergence operator with respect to velocity. The discrete particle acceleration is [5]

$$A = D_P(\boldsymbol{u}_f - \boldsymbol{u}_p) - \frac{1}{\rho_p}\nabla p + \boldsymbol{g} - \frac{1}{\theta_p \rho_p}\nabla \tau \quad (4)$$

Where D_P is the drag coefficient, θ_p is the particle volume fraction, ρ_p is particle density, $\boldsymbol{u}_p$ is the local mass-averaged particle velocity, τ is the gradient in the interparticle stress.

The particle volume fraction is associated with the particle distribution function and the particle force per volume in the fluid phase.

$$\theta_p = \iiint \phi \Omega_p d\Omega_p d\rho_p d\boldsymbol{u}_p \quad (5)$$

And

$$\theta_f + \theta_p = 1 \quad (6)$$

As for the drag force, the choice of drag coefficient formulation significantly contributes to improving the accuracy of numerical predictions [6]. Different drag force models have been proposed and many of them are used in CFD software [7].

In the Eulerian momentum equation,

$$\boldsymbol{F} = \iiint \phi \Omega_p \rho_p \left[D_p(\boldsymbol{u}_f - \boldsymbol{u}_p) - \frac{1}{\rho_p} \right] d\Omega_p d\rho_p d\boldsymbol{u}_p \quad (7)$$

The particle continuity equation is

$$\frac{\partial(\overline{\theta_p \rho_p})}{\partial t} + \nabla \cdot (\overline{\theta_p \rho_p}\ \overline{u_p}) = 0 \quad (8)$$

and particle momentum equation is

$$\frac{\partial(\overline{\theta_p \rho_p}\ \overline{u_p})}{\delta t} + \nabla \cdot (\overline{\theta_p \rho_p}\ \overline{u_p}\ \overline{u_p}) = -\theta_p \nabla p - \nabla \tau_p + \overline{\theta_p \rho_p}\,\mathbf{g} + \iiint \phi \Omega_p \rho_p D_p(\boldsymbol{u}_f - \boldsymbol{u}_p) d\Omega_p d\rho_p d\boldsymbol{u}_p - \nabla \cdot \left[\iiint \phi \Omega_p \rho_p (\boldsymbol{u}_p - \overline{\boldsymbol{u}_p})(\boldsymbol{u}_p - \overline{\boldsymbol{u}_p}) d\Omega_p d\rho_p d\boldsymbol{u}_p \right] \quad (9)$$

Where the mean particle velocity $\overline{u_p}$ is given by

$$\overline{u_p} = \frac{1}{\overline{\theta_p \rho_p}} \iiint \phi \Omega_p \rho_p \boldsymbol{u}_p d\Omega_p d\rho_p d\boldsymbol{u}_p \quad (10)$$

And the average particle density is given by

$$\overline{\theta_p \rho_p} = \iiint \phi \Omega_p \rho_p d\Omega_p d\rho_p d\boldsymbol{u}_p \quad (11)$$

3. Simulation conditions

3.1 pressure

To decide the inlet pressure of the cyclone, that is, the source term pressure, Table I and Table II showed the current design pressure and the rupture pressure of the containment. In the applied scenario of the proposed filtration system, 200 kPa was chosen because there would be a tank to collect the source term as a cushion before input it to the cyclone part. The outlet pressure should be higher than the environment pressure, thus is chosen as 150 kPa.

Table I: Containment Designed Pressure [8]

	Design Pressure(psig/kPa)
BWR Mark I	62/427
BWR Mark	12/83
BWR Mark	15/103
PWR Sub-atmospheric	45/310
PWR Large Dry	60/414

Table II: Best Estimate of Rupture Pressure for the Sequoyah Containment from Various NRC- sponsored Studies [9]

Reference	Date	Rupture pressure (psig/kPa)	Method of Analysis and Rupture Locations
NUREG/CR-5405	1990	63/434	*
NUREG/CR-6706	2001	68(62-74)/469	**
NUREG/CR-6920	2006	67(54-82)/462	***

* Finite element analysis Rupture location: where the containment shell thickness abruptly increases around the larger containment openings in the ice condenser region of the containment.

** Finite element analysis Rupture location: as above.

*** Finite element analysis Containment fragility provided lower and upper bounds corresponding to 0.05 and 0.95 probabilities of failure Rupture location: as above.

3.2 Cyclone

The cutoff aerodynamic diameter of a cyclone is usually greater than 5 to 10 μm, and therefore it is often used as a precollector in front of other high-efficiency devices [10].

The Stairmand-type high efficiency cyclone was first mentioned by Stairmand (1951). It is one of the standard cyclone designs and is most commonly used. After checking the height limit of US and China and South Korea, for transportation convenience, D=1 is chosen. Thus the geometry of the cyclone is shown as follows.

Tale III: Geometry of the cyclone

Cyclone	a/D	b/D	D_x/D	H_t/D	h/D	S/D	B_c/D
Staimand design	0.5	0.2	0.5	4	1.5	0.5	0.375

The flow Reynolds numbers in industrial cyclones are frequently 3×10^5 or higher [11]. The cutoff diameter of the cyclone, Dp_{50}, is defined as the particle diameter corresponding to 50% collection efficiency. It is an indicator of the size range of particles that can be collected.(Lapple, 1950). The cutoff diameter derived by Lapple (1950) is as [10]

$$D_{p50} = 3\sqrt{\frac{\mu b}{2\pi\rho_p U_i C N_t}}$$

Where U_i is the gas velocity at the inlet; μ is the air dynamic viscosity; ρ_p is the particle density; C is the slip correction factor of the particle corresponding to D_{p50}. The number of turns N_t can be calculated as $N_t = tU_i/\pi D$ and the residence time t is equal to the volume of the cyclone divided by the volumetric flow rate, Q. The cyclone in this application is assumed to be the industry high speed cyclone. The maxim speed range is from 1000 rmp/min to 15000 rmp/min according to the inlet flow.

3.3 Model

Thus, the design parameters are listed below:

Table IV: Parameters of the cyclone simulation conditions

Parameter	Sign	Value
Flow speed	v(m/s)	15
Turbulence degree		5%
Rotation speed	n(rpm/min)	10000-15000
Inlet pressure	p(kPa)	200
Outlet pressure	P(kPa)	150
Inlet temperature	T_i(K)	300
Particle diameter [12]	d_p(mm)	0.1-0.5
Particle density	ρ_p(g/m^3)	0.1-100

The LES model is used, and the model and mesh of the cyclone part is shown below.

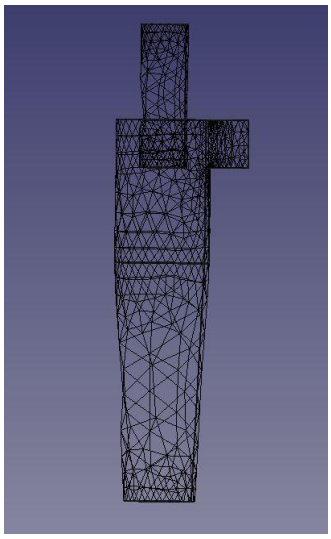

Fig. 2. Cyclone part mesh generation

Because the standard Stairmand cyclone is applied in this paper, the separation efficiency can be predicted.

For our simulation condition, $\mu = 1.846\times10^{-5}$ kg·m^{-1}·s^{-1}, particles are in the range of 0.1-0.5 mm, particle density is chosen as 50 g/m3 for the cutoff diameter calculation, C is set as 1[13]. According to calculation, N_t is equal to 19.73, thus 20 is chosen. So Dp50 can be calculated as 0.00265m, which is much bigger than the particle diameter, thus the separation efficiency will be relatively low. Further comparison of the theoretical and simulation separation efficiency will be conducted.

After the cyclone part as a pre-filter, the gaseous part, which consist of noble gas and I_2, can be collected by the upper part filters. Activated carbon is widely used for removing iodine from relatively benign gaseous streams, e.g. impregnated activated carbon is used almost exclusively for gaseous radioiodine removal at nuclear power plants (Jubin 1988).

For the lower part, the CsI may be the main concern according to the source term analysis. Alkaline scrubber will be used to capture it.

Future work

Further simulation analysis and modification of the cyclone and the absorbent/filtration will be analysis to evaluate the whole efficiency of this system.

REFERENCES

[1] M.L.Ang, A.Meyer-Heine et al., A Comparison of World-Wide Uses of Severe Reactor Accident Source Terms, Sep. 1994

[2] D.M. Snider, An incompressible 3D multiphase PIC model for dense particle flow, Journal of Computational Physics 170, pp. 523-549, 2001.

[3] M.J. Andrews, P. J. O'Rourke, The Multiphase Particle-in-Cell (MP-PIC) Method for Dense Particulate Flows, Int. J. Multiphase Flow, Vol.22, pp.379-402, 1996
[4] F. A. Williams, Combustion Theory, 2nd ed. Benjamin–Cummings, Menlo Park, CA, 1985.
[5] M. J. Andrews and P. J. O'Rourke, The multiphase particle-in-cell (MP-PIC) method for dense particle flow, Int. J. Multiphase Flow 22, 379, 1996.
[6] Mohsen Karimi, Guven Akdogan, Comparison of Different Drag Coefficient Correlations in the CFD Modelling of a Laboratory-scale Rushton-turbine Flotation tank.
[7] Joachim Lundberg, Britt M. Halvorsen, A Review of Some Existing Drag Models Describing the Interaction Between Phases in a Bubbling Fluidized Bed,
[8] Dave Lochbaum, Nuclear Plant Containment Failure: Overpressure, allthingsnuclear.org, May, 2016
[9] State of the Art Reactor Consequence Analyses (SOARCA) Project, U.S.NRC
[10] Kung-Yu Kuo, Chuen-Jinn Tsai, On the Theory of Particle Cutoff Diameter and Collection Efficiency of Cyclones, Aerosol and Air Quality Research, Vol.1, No.1, pp.47-56, 2001.
[11] Murry E. Moore, Andrew R. McFarland, Performance Modeling of Single-Inlet Aerosol Sampling Cyclones, Environ. Sci. Technol., 27, pp.1842-1848, 1993.
[12] Tim Haste, Severe accident phenomena part 2: Ex-vessel, IAEA Workshop on Severe Accident Management Guidelines, 19-23 Oct. 2015, Vienna, Austria
[13] Finlayson-Pitts, B. J., and J. N. Pitts, 2000: Chemistry of the Upper and Lower Atmosphere: Theory, Experiments and Applications. Academic Press, 363.